The Urokinase Receptor-Derived Peptide UPARANT Recovers Dysfunctional Electroretinogram and Blood–Retinal Barrier Leakage in a Rat Model of Diabetes

Maurizio Cammalleri,[1] Filippo Locri,[1] Stefania Marsili,[1] Massimo Dal Monte,[1] Claudio Pisano,[2] Angelo Mancinelli,[2] Liliana Lista,[3] Dario Rusciano,[4] Mario De Rosa,[5] Vincenzo Pavone,[3] and Paola Bagnoli[1]

[1]Department of Biology, University of Pisa, Pisa, Italy
[2]Medicinal Investigational Research, Biogem Research Institute, Ariano Irpino, Italy
[3]Department of Biology, University of Napoli Federico II, Napoli, Italy
[4]Sooft Italia Spa, Montegiorgio, Italy
[5]Department of Experimental Medicine, Second University of Napoli, Napoli, Italy

Correspondence: Paola Bagnoli, Department of Biology, University of Pisa, Via San Zeno 31, Pisa 56127, Italy;
paola.bagnoli@unipi.it.

Submitted: February 1, 2017
Accepted: May 10, 2017

Citation: Cammalleri M, Locri F, Marsili S, et al. The urokinase receptor-derived peptide UPARANT recovers dysfunctional electroretinogram and blood–retinal barrier leakage in a rat model of diabetes. *Invest Ophthalmol Vis Sci*. 2017;58:3138–3148. DOI: 10.1167/iovs.17-21593

Purpose. The activation of the urokinase-type plasminogen activator and its receptor system is associated with retinal diseases. Among peptide inhibitors of this system, UPARANT acts by preventing the onset of pathologic signs of neovascular ocular diseases. We investigated whether systemic UPARANT may act in a therapeutic regimen by suppressing the retinal damage that characterizes diabetic retinopathy using a rat model of streptozotocin-induced diabetes.

Methods. In healthy rats, plasma, eye, and retina concentrations of UPARANT were evaluated by mass spectrometry. In rat models of streptozotocin-induced diabetes, the appearance of diabetic retinopathy was assessed by electroretinogram (ERG). UPARANT was then administered at different dosages and daily regimens. ERG recording, Evans blue perfusion, and real-time PCR were used to evaluate UPARANT efficacy. UPARANT safety was also determined.

Results. UPARANT was found in plasma, eye, and retina soon after its administration and remained detectable after 24 hours. Between the 4th and the 5th week after diabetes onset, UPARANT at 8 mg/kg (daily for 5 days) was effective in recovering dysfunctional ERG. Three-day treatments at 8 mg/kg or a half dose for 5 days were ineffective. ERG recovery lasted approximately 2 weeks. ERG recovery was accompanied by restored blood–retinal barrier integrity and inhibition of inflammatory and angiogenic responses. UPARANT showed a safety profile.

Conclusions. These data suggest that targeting the urokinase-type plasminogen activator and its receptor system by systemic UPARANT is a potential therapeutic approach for the treatment of early diabetic retinopathy, thus providing a potential alternative approach to delay disease progression in humans.

Keywords: inflammatory factors, proangiogenic factors, streptozotocin

Diabetic retinopathy (DR), one of the leading causes for vision loss in the Western world, is a complication caused by high blood sugar that activates several complex interconnecting pathways. Inflammatory and proangiogenic factors play a prominent role in increasing the vascular permeability that characterizes the early phase of DR.[1,2] Vascular endothelial growth factor (VEGF), which is the major growth factor mediating vascular leakage, accumulates very early during DR[3] and its inhibition at later stages is mostly intended to regulate excessive vasopermeability and consequent diabetic macular edema.[4] However, current anti-VEGF therapies, although effective to a certain level, do not always ameliorate vision impairment,[5] have only limited impact on inflammatory processes,[6] require prolonged treatment regimens with frequent intravitreal injections and, consequently, carry some risks.[7] Current therapeutic strategies have suboptimal efficacy, and disease progression often continues despite pharmacologic interventions.[6,8]

Newer multitarget drugs directed to key mediators of microvascular damage, including a multitude of inflammatory and proangiogenic factors, may be an effective approach to treat DR at an early stage and prevent its progression.

Among the several pathways known to be involved in DR, the system formed by urokinase-type plasminogen activator (uPA) and its receptor (uPAR) is particularly attractive because it is a major player in diabetes-induced blood–retinal barrier (BRB) breakdown.[9–11] Being devoid of intracellular domains, uPAR activates intracellular signaling cascades by lateral interactions with other components of the cellular membrane, including the formyl peptide receptors (FPRs).[12] uPAR is mostly

localized to retinal endothelial cells[9,10] and pigment epithelial cells.[13] Increased levels of uPA/uPAR are associated with proliferative DR in humans[14,15] and early DR in rodent models.[9,10] uPA/uPAR levels increase in retinal endothelial cells in response to both oxidative stress and VEGF increase caused by high glucose, generating a proteolytic cascade that has detrimental effects on cell permeability.[10,11,16–19] In addition, upregulated uPA/uPAR would result in the increased expression of extracellular metalloproteinases[9] and intracellular effectors[20] that concur to BRB breakdown.

Deletion of the uPAR gene or treatment with A6, a compound that affects the interaction of uPA/uPAR with other cell surface proteins, prevents BRB breakdown in rodent models of DR.[10,11] The recently synthetized tetrapeptide UPARANT displays lasting resistance to enzymatic digestion and high stability in blood and plasma.[21] UPARANT has been designed to mimic the sequence ^{88}Ser-Arg-Ser-Arg-Tyr^{92}, through which uPAR interacts with FPRs. Accordingly, UPARANT competes with N-formyl-Met-Leu-Phe, a known FPR ligand, for binding to FPRs. UPARANT has been found to reduce VEGF-induced angiogenesis both in vitro and in vivo.[16,21,22] In particular, in mouse models of neovascular ocular pathologies, intravitreal administration of UPARANT prevents the onset of neovascularization and BRB leakage through the inhibition of proangiogenic and inflammatory factors and also prevents electroretinogram (ERG) dysfunction.[20,22]

In the present study, we investigated the effect of systemic UPARANT in a therapeutic setting on diabetes-induced early DR using streptozotocin-treated rats (STZ-rats). The STZ-rat model recapitulates the initial process of DR in humans, including increased levels of inflammatory and proangiogenic factors and retinal vasopermeability, thus causing BRB breakdown and ERG alterations (for references, see Ref. 23), although different susceptibility to the effects of STZ have been described in different strains of rats.[24–26] In the STZ-model, neither macular edema or proliferative disease ever develop; however, results on the efficacy of therapeutic agents have often been used as the sole preclinical data underlying clinical studies in human with diabetic macular edema.[27] Here, the possibility that systemic UPARANT reaches the retina was first tested in healthy rats. Then ERG recordings served to evaluate the effectiveness of UPARANT in terms of either dosing or treatment duration. BRB integrity was evaluated as a sign of potential efficacy of UPARANT in recovering normal vessel permeability. Inflammatory and proangiogenic factors were also determined to identify the potential targets of the drug. Finally, the safety of subcutaneous UPARANT was also evaluated.

Materials and Methods

UPARANT was synthesized as previously described.[21] The RNeasy Mini and QuantiTect Reverse Transcription kits were purchased from Qiagen (Valencia, CA, USA). The PCR master mix (SsoAdvanced Universal SYBR Green Supermix) and the iScript One-Step RT-PCR kit with SYBR Green were from Bio-Rad Laboratories (Hercules, CA, USA). Primers were obtained from Eurofins (Ebersberg, Germany). All other chemicals were obtained from Sigma-Aldrich Corp. (St. Louis, MO, USA).

Animals and UPARANT Treatment

Sprague-Dawley rats (107 males, 150–200 g) were obtained from Charles River Laboratories, Italia (Calco, Italy). Of them, 25 rats were used for the pharmacokinetics (PK) study and 6 for the safety study. Of the remaining 76 rats, 70 were treated with a single intraperitoneal injection of 65 mg/kg STZ to induce diabetes, and 6 received a single intraperitoneal injection of citrate buffer at pH 4.5 (from now on referred to as *controls*). In STZ-treated rats, blood glucose was measured by tail sampling using a One Touch Ultra glucometer (LifeScan, Inc., Mipitas, CA, USA) 3 days after treatment then weekly thereafter. Rats with blood glucose values >250 mg/dL were considered diabetic. UPARANT was dissolved in PBS and the treatment was initiated after 4 weeks when diabetic rats demonstrated significantly dysfunctional ERG. Of the diabetic rats, 6 received UPARANT at 8 mg/kg daily for 3 days, 20 received UPARANT at 8 mg/kg daily for 5 days, 6 received UPARANT at 4 mg/kg daily for 5 days, 20 received PBS and 18 were left untreated. In all experiments, rats were anesthetized with an intraperitoneal injection of pentobarbital (30 mg/kg). Procedures involving animals were carried out in agreement with the ARVO Statement for the Use of Animals in Ophthalmic and Vision Research and in compliance with the Italian guidelines for animal care (DL 116/92) and the European Communities Council Directive (86/609/EEC). Procedures were approved by the Ethical Committee in Animal Experiments of the University of Pisa.

Pharmacokinetics Study

Rats received a single dose of subcutaneous UPARANT (20 mg/kg in PBS). This dose derives from the finding that in a mouse model of AMD, choroidal neovasclarization was inhibited by subcutaneous administration of UPARANT at 40 mg/kg,[20] a dose corresponding here to 20 mg/kg if one considers the body surface area normalization method that allows to appropriately translate the drug dosage from one animal species to another.[28] Of the 25 rats used for the PK study, 5 were used for plasma PK, 10 for eye distribution, and 10 for retina distribution. For plasma PK, blood was collected at different time points (0.25, 0.5, 1, 2, 4, 6, 8, and 24 hours after dose), whereas for tissue distribution eyes and retinas were collected at 2 hours and 24 hours postdosing. Blood was drawn into sodium-heparinized test tubes and centrifuged (5 minutes, 6000*g* at 4°C), and the resultant plasma stored at −20°C. The plasma (50 μL) was added to 1% formic acid in methanol (300 μL), then vortex mixed for 1 minute, stored at −20°C for 20 minutes, vortex mixed for 30 seconds, and centrifuged at 12,000*g* for 10 minutes at 4°C. Finally, a 100-μL aliquot of the resultant supernatant was transferred into autosampler vials, and a 3-μL aliquot was analyzed. For tissue distribution, eyes or retinas were homogenized in MilliQ water (Millipore, Billerica, MA, USA) in a 1:5 ratio (tissue weight:volume). Then a 100-μL aliquot was added with 300 μL of 1% formic acid in methanol and processed as described previously. Calibration curve (0.05–2.0 μg/mL) and quality control samples (0.08 and 1.6 μg/mL) were prepared in plasma or homogenized tissues of rats that received PBS. In rats that received UPARANT, drug concentration in the plasma, eyes, or retinas was determined with a U-HPLC instrument (UltiMate 3000; ThermoScientific, Bremen, Germany) coupled to an Orbitrap high-resolution mass spectrometer (Exactive; ThermoScientific). Data acquisition was under the control of Xcalibur software version 2.1 (ThermoScientific). Chromatography was performed using a gradient system consisting of mobile phase solution A (0.3% formic acid in water) and solution B (methanol) with a flow rate of 0.5 mL/min at room temperature. The gradient elution method was as follows: 0 to 2 minutes 90% A, 2 to 4 minutes 10% A, 4 to 6 minutes 10% A, 6 to 7 minutes 90% A, 7 to 10 minutes 90% A. The calibration curves were linear over the concentration range considered with a correlation coefficient > 0.99. The lower limit of quantification (LLOQ) measured with acceptable accuracy and precision (≤20%) was 0.05 μg/

mL. Accuracy of quality control samples was lower than −10.5%. The maximum concentration (C_{max}) and the time to reach C_{max} (t_{max}) were obtained from data above the LLOQ. The apparent elimination rate constant (K_{elim}) was calculated as the negative slope of the log-linear terminal portion of the plasma concentration-time curve using linear-regression. A minimum of three observations was used to calculate K_{elim}. The half-life was calculated as $0.693/K_{elim}$. The area under the curve (AUC) was calculated by linear trapezoidal rule and extrapolated to infinity using the terminal slope and the last plasma concentration.

Electroretinographic Recording

Retinal function was examined with scotopic full-field ERG. Before ERG testing, rats were dark adapted overnight. In anesthetized rats, pupils were dilated with 0.5% atropine, the cornea was intermittently irrigated with saline solution to prevent clouding of the ocular media, and a heating pad was used to keep the body temperature at 38°C. The ERG responses were recorded through silver/silver chloride corneal electrodes and a forehead reference electrode, and a ground electrode was placed on the tail. Scotopic ERG, which primarily measures rod function, was evoked by flashes of different light intensities ranging from −3.4 to 1 log cd-s/m^2 generated through a Ganzfeld stimulator (Biomedica Mangoni, Pisa, Italy). The electrodes were connected to a two-channel amplifier. Signals were amplified at 1,000 gain and bandpass filtered between 0.2 and 500 Hz before being digitized at 5 kHz rate with a data acquisition device (Biomedica Mangoni). The ERG waveforms were examined primarily for amplitude information (i.e., the size of the a- and b-waves), and the data were graphed to determine any gross changes in the intensity-response function for that eye. Data were pooled and reported as mean amplitude ± SEM (in μV). Intensity-response functions of the b-wave were fit to the following modified Naka-Rushton function[29]:

$$V(I) = V0 + (Vmax\ In)/(In + kn).$$

In this equation, V is the amplitude of the b-wave (in μV), I is the stimulus intensity (in log cd-s/m^2), V0 is the nonzero baseline effect, Vmax is the saturated amplitude of the b-wave (in μV), and k is the stimulus intensity that evokes a b-wave of half-maximum amplitude (in log cd-s/m^2); n, which was constrained to unity, is a dimensionless constant controlling the slope of the function and represents the degree of heterogeneity of retinal sensitivity.

Measurement of Retinal Vascular Leakage by Evans Blue Dye

Diabetes-induced leakage from the retina was evaluated by assessment of Evans blue dye extravasation. Briefly, anesthetized rats were injected with Evans blue dye (0.5% in PBS) into the left ventricle and allowed to circulate for 10 minutes. For quantitative evaluation of BRB leakage, the animals were euthanized, and the eyes were enucleated and the retinas isolated and weighted. The Evans blue dye was extracted with formamide overnight at 65°C, read at 620 nm (the absorbance maximum for Evans blue) using a plate reader (Microplate Reader 680 XR; Bio-Rad Laboratories). Evans blue leakage was expressed as the percentage of the absorbance in controls. For qualitative evaluation of outer BRB leakage, enucleated eyes were fixed in 4% paraformaldehyde and the retinas were flat mounted and examined with a fluorescence microscope (Ni-E; Nikon Europe, Amsterdam, The Netherlands), and images were acquired (DS-Fi1c camera; Nikon Europe). For each experimental condition, six retinas from six different rats were used.

Measurement of Inflammatory and Proangiogenic Markers by Quantitative Real-Time PCR (qRT-PCR)

Relative Quantification. To perform qRT-PCR experiments, six samples, each containing one retina, were used for each experimental condition. Total RNA was extracted using an isolation kit (RNeasy Mini Kit; Qiagen), purified, resuspended in RNase-free water, and quantified using a fluorometer (Qubit; Invitrogen, Carlsbad, CA, USA). First-strand cDNA was generated from 1 μg of total RNA (QuantiTect Reverse Transcription Kit; Qiagen). RT-PCR amplification was performed with a kit (SsoAdvanced Universal SYBR Green Supermix; Bio-Rad Laboratories) on a Miniopticon Real Time PCR System and software CFX manager (Bio-Rad Laboratories). qRT-PCR primer sets for inflammatory and proangiogenic markers, including interleukin-1β (IL-1β), IL-6, the inducible form of nitric oxide synthase (iNOS), intercellular adhesion molecule-1 (ICAM-1), glial fibrillary acidic protein (GFAP), VEGF, insulin-like growth factor-1 (IGF-1), fibroblast growth factor-2 (FGF-2), platelet-derived growth factor-B (PDGF-B) and angiopoietin-2 (Ang-2) were chosen to hybridize to unique regions of the appropriate gene sequence (see Supplementary Table S1 for complete list of assayed genes and primers). Amplification efficiency was close to 100% for each primer pair (Opticon Monitor 3 software; Bio-Rad Laboratories). Target genes were assayed concurrently with *18S*, a constitutively expressed gene encoding 18S ribosomal RNA, widely used as housekeeping gene in DR studies (for instance, see Ref. 30). Samples were compared using the relative threshold cycle (Ct Method). The increase or decrease (fold change) was determined relative to control rats after normalization to *18S*. All reactions were performed in triplicate. After statistical analysis, the data from the different experiments were plotted and averaged in the same graph.

Absolute Quantification. To determine absolute messenger RNA (mRNA) levels of inflammatory and proangiogenic factors, their transcription was examined using absolute qRT-PCR. To quantify gene expression, an absolute standard curve method was used. Briefly, the standard curves were generated using genomic DNA obtained from the retinas of three healthy rats. The extraction of genomic DNA was performed using a QIAamp DNA Mini Kit (Qiagen). Genomic DNA was quantified by a spectrophotometer (BioSpectrometer fluorescence, Eppendorf, Hamburg, Germany), and the DNA copy number was calculated. For standard curve acquisition, seven serial dilutions of genomic DNA from 90,000 to 5.4 copies were prepared and quantified using a kit (iScript One-Step RT-PCR kit with SYBR Green; Bio-Rad Laboratories) and appropriate primers (Supplementary Table S2). The RNA samples (30 ng) were amplified in parallel with genomic DNA standards and their CT values were plotted together with those of the genomic DNA, from which the normalized mRNA copy numbers were determined. The values were expressed as the number of mRNA copies relative to the number of copies of hypoxantine phosphoribosyl transferase used as a housekeeping gene. All reactions were run in triplicate. After statistical analysis, the data from the different experiments were averaged.

Safety Study

The study was carried out in rats treated with UPARANT at 10 mg/kg ($n = 3$) daily for 7 days, a dose and a treatment duration slightly higher than those used to evaluate the effects of UPARANT on the pathologic signs of STZ-induced DR. Three

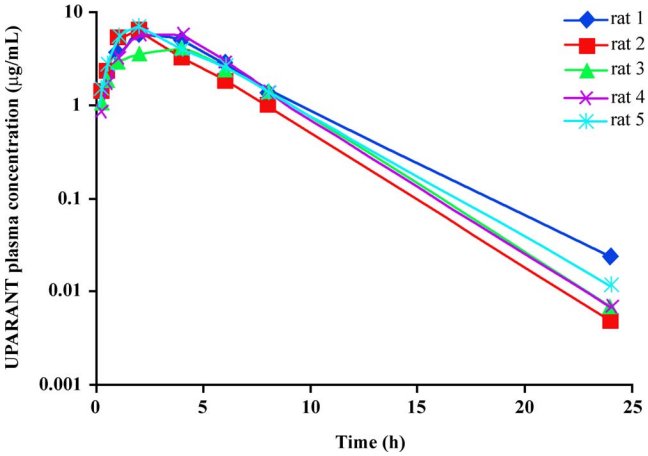

Figure 1. Pharmocokinetics profile of UPARANT. UPARANT was administered subcutaneously as a single shot at 20 mg/kg. Plasma samples were assayed for UPARANT using HPLC-MS. C_{max} was observed 2 hours after administration. At 24 hours after administration, UPARANT still remained detectable in the plasma. The data represent UPARANT concentration in the plasma of each rat used in the study (n = 5). See the Table for full PK parameters.

rats received PBS. Body weight was recorded at the beginning and the end of the study when the rats were fasted overnight to be then anesthetized for blood collection and necropsy. Blood was collected in two different tubes: one tube containing the anticoagulant EDTA for hematologic examination and one tube without anticoagulant for biochemical examination. Blood collected in EDTA-coated vials was analyzed using an automatic hematology analyzer (Vetscan HM5C Analyzer; Abaxis, Dunnington, UK) shortly after its collection. Blood samples collected in tubes lacking anticoagulant were placed at room temperature for at least 90 minutes prior to centrifugation to collect serum that was used to evaluate biochemical parameters with a fully automated random access clinical chemistry analyzer (VitroVet; scil animal care GmbH, Viernheim, Germany). After blood collection, the animals were killed. Vital organs were excised, and their gross morphology was examined for macroscopic features. In addition, we evaluated the potential histopathologic alterations of liver and kidney, the most important organs for detoxification processes. To this aim, the organs were removed, formalin fixed, paraffin embedded, and then cut into 4-μm sections and stained with hematoxylin and eosin according to standard protocols. Digital photomicrographs were taken using an imaging system of light microscope equipped with a digital camera.

Data Analysis

Statistical significance was evaluated using 1-way analysis of variance (ANOVA) followed by Newman–Keuls' multiple comparison posttest or 2-way ANOVA followed by Bonferroni's multiple comparison posttest as appropriate. The results are expressed as mean ± SEM of the indicated n values (Prism 5; GraphPad Software, San Diego, CA, USA). Differences with $P < 0.05$ were considered significant.

Results

Plasma, Eye, and Retina Levels of UPARANT

As shown in Figure 1, subcutaneously administered UPARANT rapidly appeared in the plasma being quantifiable at 0.25 hours, reached the C_{max} (5.9 ± 1.2 μg/mL) at 2 hours, and declined following a monophasic profile. UPARANT was still detectable at 24 hours, when its level reached values that, although below the LLOQ, were statistically different from the blank. These values are represented in Figure 1, but were not considered in evaluating PK parameters in agreement with the Food and Drug Administration Guidance on Bioanalytical Method Validation.[31] UPARANT was cleared from the plasma with a $t_{1/2}$ of 3 hours. Additional pharmacokinetics parameters of plasmatic UPARANT are summarized in the Table.

Table. Pharmacokinetic Parameters of UPARANT

K_{elim}, h	$t_{1/2}$, h	C_{max}, ug/mL	t_{max}, h	AUC_{last}, ug-h/mL	AUC_{info}, ug-h/mL
0.24 ± 0.06	3.0 ± 0.90	5.9 ± 1.2	2.0	28.5 ± 3.4	34.4 ± 3.1

K_{elim}, apparent elimination rate constant was calculated as negative slope of the log-linear terminal portion of the plasma concentration-time curve using linear-regression; $t_{1/2}$, terminal half-life; C_{max}, maximum plasma concentration; t_{max}, time of C_{max}; AUC_{last}, area under the concentration versus time curve from 0 to t_{last}; AUC_{inf}, area under the concentration versus time curve from 0 to infinity.

At 2 hours postdosing, UPARANT concentration in the eye was 1.10 ± 0.20 μg/g, whereas in the retina it was 0.16 ± 0.02 μg/g. At 24 hours, UPARANT remained still detectable in the eye (0.22 ± 0.03 μg/g, a value that was four times higher than the LLOQ) and in the retina (0.04 ± 0.02 μg/g, a value slightly below the LLOQ).

UPARANT Efficacy on ERG Dysfunction and BRB Leakage

The efficacy of UPARANT on retinal dysfunction that characterizes early DR was investigated in a longitudinal ERG monitoring in which 24 rats, randomly chosen, were recorded at different times after diabetes onset. Representative ERG recordings shown in Figure 2 demonstrate that at 2 weeks, ERG amplitude was similar to that of controls, whereas at the 4th week, ERG became dysfunctional, in line with previous findings (for references, see Ref. 32). ERG dysfunction persisted after 3 days of treatment with 8 mg/kg UPARANT, but recovery was observed after 5 days. Restored ERG persisted for approximately 2 weeks after UPARANT withdrawal, when ERG became again dysfunctional. Rats receiving 4 mg/kg UPARANT for 5 days did not exhibit any recovery (not shown).

ERG analysis was performed after 5 days administration of 8 mg/kg UPARANT. Figure 3A shows representative mixed a- and b-waves recorded at light intensities of 1 log cd-s/m^2. No differences in a- and b-waves were observed between diabetic untreated and diabetic vehicle-treated rats. An increase in a- and b-wave amplitudes with increasing stimulus intensity was observed. A clear a-wave developed at a light intensity of approximately −1.6 log cd-s/m^2. With respect to controls, untreated or vehicle-treated diabetic rats showed a reduction in the amplitude of both the a-wave (at light intensities ranging from −0.3 to 1 log cd-s/m^2; $P < 0.01$; Fig. 3B) and the b-wave (at light intensities ranging from −2.8 to 1 log cd-s/m^2; $P < 0.001$; Fig. 3C). UPARANT recovered the amplitude of the a- and b-waves to values that did not significantly differ from those in controls (Fig. 3). When evaluating the b-wave amplitude with a fitted Naka-Rushton function, the response amplitude (Vmax) and the retinal sensitivity (k) of untreated or vehicle-treated diabetic rats were significantly lower than in controls with Vmax of 534.9 ± 30.7 μV and k of −0.3 ± 0.2 log cd-s/m^2 with respect to Vmax of 764.2 ± 19.60 μV and k of

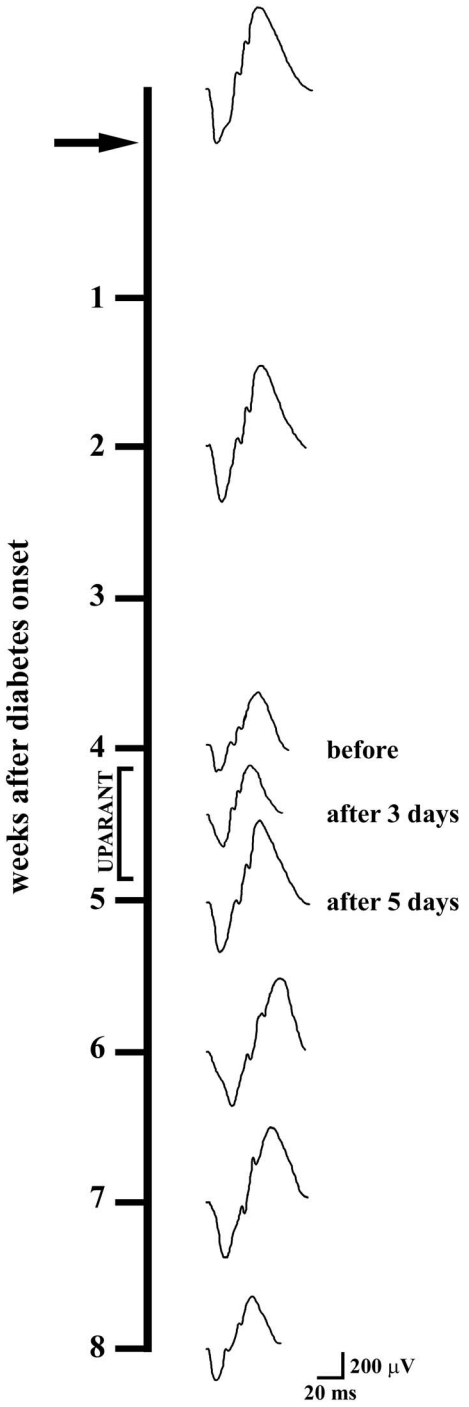

FIGURE 2. Schematic representation of longitudinal ERG monitoring either before or at different times after diabetes onset. The *arrow* indicates the day of diabetes onset. ERG was recorded in each rat at the indicated time points. At 2 weeks after diabetes onset, ERG amplitude was similar to that of controls, whereas at the 4th week ERG became dysfunctional. ERG monitoring performed after UPARANT administration demonstrates that ERG amplitude recovered to normal value after 5 days treatment with subcutaneous UPARANT at 8 mg/kg. At 3 days, treatment did not influence the dysfunctional ERG. Restored ERG persisted for approximately 2 weeks (6th and 7th week after diabetes onset) after which ERG became again dysfunctional (8th week after diabetes onset).

−1.57± 0.15 log cd-s/m^2 ($P < 0.001$). After UPARANT, the values of Vmax and k were not significantly different from those in controls, with Vmax of 736.1 ± 19.06 μV and k −1.38 ± 0.14 log cd-s/m^2.

To investigate whether ameliorated ERG may depend on restored BRB integrity, we evaluated BRB leakage by measuring the extravasation of Evans blue, a dye that binds to plasma proteins. In diabetic rats either untreated or vehicle treated, Evans blue dye leakage was increased by approximately 2.3-fold with respect to controls ($P < 0.001$; Fig. 4A). UPARANT recovered this increase to a level close to controls. Qualitative evaluation of the BRB integrity demonstrated that, when compared with controls (Fig. 4B), untreated (Fig. 4C) or vehicle-treated (Fig. 4D) diabetic rats showed a clear extravasation of Evans blue bound to circulating proteins. BRB breakdown was reduced by UPARANT as evidenced by the decrease of dye leakage into the retinal parenchyma (Fig. 4E).

UPARANT Efficacy on Inflammatory and Proangiogenic Markers

Untreated diabetic rats displayed mRNA levels of IL-1β (Fig. 5A), IL-6 (Fig. 5B), iNOS (Fig. 5C), ICAM-1 (Fig. 5D), and GFAP (Fig. 5E) that were higher than in controls (approximately 4.2-, 2.8-, 2.2-, 3.6-, and 3.0-fold, respectively; $P < 0.001$). In addition, mRNA levels of VEGF (Fig. 6A), IGF-1 (Fig. 6B), FGF-2 (Fig. 6C), PDGF-B (Fig. 6D), and Ang-2 (Fig. 6E) were increased by approximately 2.2-, 2.3-, 5.8-, 2.3-, and 2.3-fold, respectively ($P < 0.001$). A similar increase was also found in vehicle-treated diabetic rats. UPARANT reduced inflammatory and proangiogenic transcripts with a trend toward recovering the levels found in controls. IL-1β, IL-6, iNOS, and GFAP diminished by approximately 1.5- ($P < 0.001$), 1.3- ($P < 0.05$), 1.4.- ($P < 0.001$), and 1.4-fold ($P < 0.001$) with respect to untreated or vehicle-treated diabetic rats, whereas VEGF, IGF-1, FGF-2, and PDGF-B diminished by approximately 1.5-, 1.4-, 1.7-, and 1.4-fold with respect to untreated or vehicle-treated diabetic rats, respectively ($P < 0.001$). After UPARANT, levels of ICAM-1 and Ang-2 did not significantly differ from those in controls. These patterns of gene expression were also confirmed using absolute quantification with qRT-PCR (Supplementary Table S3). Absolute mRNA levels of the analyzed factors were increased between 2.0- and 5.0-fold in untreated diabetic rats. UPARANT reduced these levels with a trend toward recovering their control values.

Safety Assessments of Systemic UPARANT

Body weight did not differ between vehicle- and UPARANT-treated rats (180 ± 5.61 g and 192 ± 2.96 g, respectively). Hematologic and biochemical parameters of vehicle- and UPARANT-treated rats are shown in Supplementary Tables S4 and S5. UPARANT did not affect significantly hematologic and biochemical parameters. In particular, the markers of liver function (aspartate aminotransferase, alanine aminotransferase, alkaline phosphatase, and total bilirubin) and those of kidney function (creatinine and blood urea nitrogen) were not influenced by UPARANT. In addition, UPARANT did not affect the gross morphology of adrenal glands, aorta, brain, cerebellum, eyes, esophagus, heart, intestine, kidneys, liver, limph nodes (cervical), lungs, mesenteric tissue, pancreas, pituitary, spleen, stomach, submaxillary glands, skin, thymus, thyroid gland, tibial bone marrow, trachea, and urinary bladder (not shown). No histopathologic alterations were found by analyzing hematoxylin/eosin stained sections of liver and kidney (Supplementary Fig. S1).

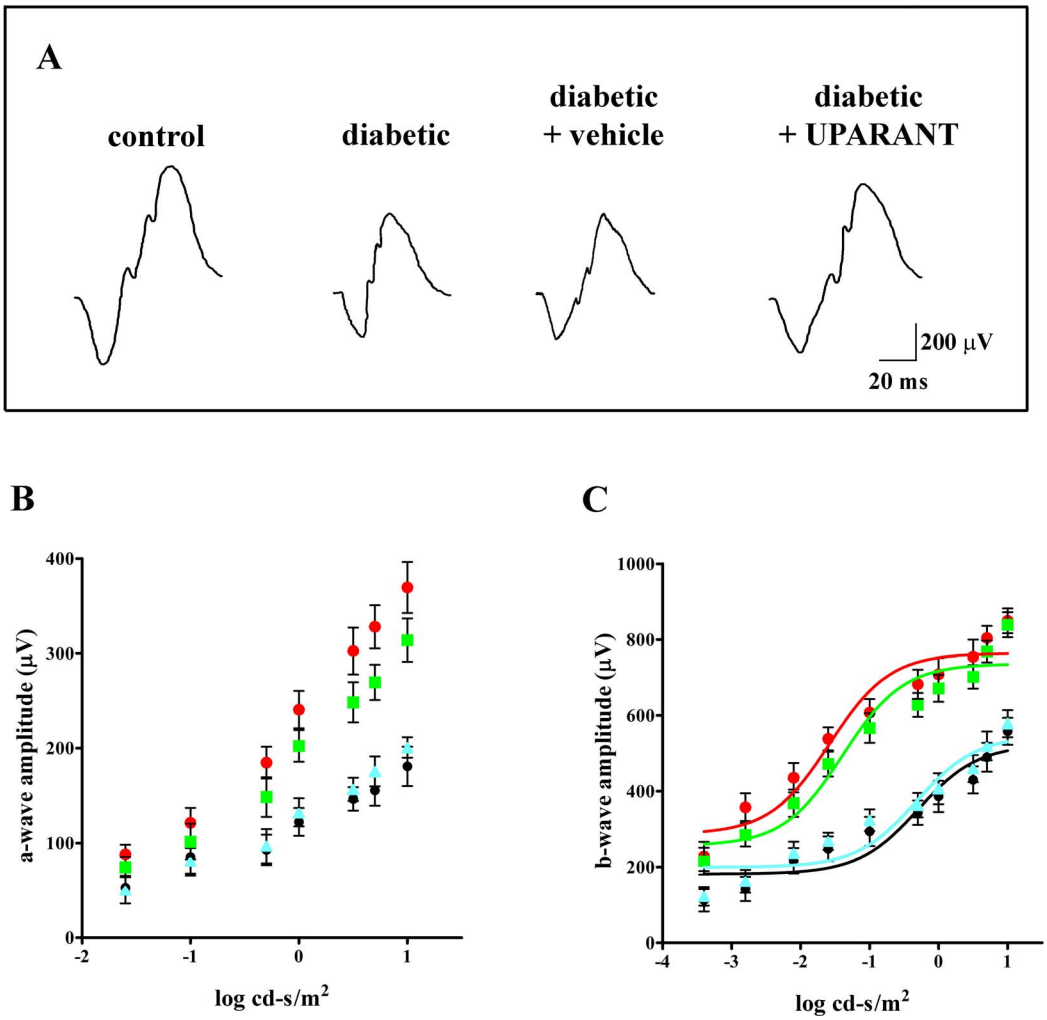

FIGURE 3. UPARANT restores ERG responses. (**A**) Representative ERG waveforms recorded at a light intensity of 1 log cd-s/m^2 in controls and in diabetic rats untreated, vehicle-treated, or treated with subcutaneous UPARANT at 8 mg/kg for 5 days. (**B, C**) Scotopic a-wave (**B**) and b-wave amplitudes (**C**) plotted as a function of increasing light intensity in controls (*red circles* and *red line*) and in diabetic rats untreated (*black circles* and *black line*), vehicle-treated (*light blue triangles* and *light blue line*), or treated with subcutaneous UPARANT (*green squares* and *green line*). In diabetic rats untreated or vehicle-treated, the amplitudes of a- and b-waves were lower than those in controls. UPARANT restored a- and b-waves to levels that were not significantly different from those in controls. Each point represents the mean ± SEM of data from 6 rats.

DISCUSSION

The present study characterizes for the first time the therapeutic effects of UPARANT in a rat model of DR. At variance with the currently used anti-VEGF treatments that are given when the disease has become vision threating, here UPARANT is found to counteract the early phase of DR, suggesting that the drug might help prevent DR progression. The UPARANT therapeutic effect demonstrated here supports the effectiveness of the systemic route as a convenient and less invasive delivery method.

UPARANT Delivery to the Eye and the Retina

As shown by the present results, subcutaneous UPARANT rapidly reaches the blood systemic circulation and remains detectable in the plasma at 24 hours, suggesting a slow elimination rate of the compound in line with its high plasma stability.[21] After 2 hours, UPARANT is well detected in the eye, indicating a significant drug transport presumably facilitated by influx peptide transporters widely distributed in eye tissues.[33] After 24 hours, the UPARANT level in the eye is approximately 20% of that at 2 hours, indicating a half-life of approximately 10 to 11 hours and suggesting a potential long duration of the intraocular pharmacologic effect. The present results also demonstrate an efficient delivery of the drug to the retina with UPARANT there being approximately 15% of that measured in the eye, suggesting that the drug penetrates the BRB.

Although more information is needed on UPARANT metabolism, the apparent ability of the drug to cross the BRB makes its subcutaneous delivery potentially effective in the treatment of ocular diseases. UPARANT delivery to the diabetic eye may be further facilitated by BRB breakdown that increases vascular permeability by 2- or 3-fold.[34] On the other hand, it should be considered that uPAR is expressed mainly by vascular endothelial cells,[35] therefore UPARANT could directly act on these cells to counteract leak and reduce inflammation without the need of crossing the BRB. In this respect, there is evidence that UPARANT acts on human retinal endothelial cells by preventing VEGF-induced membrane permeability.[16]

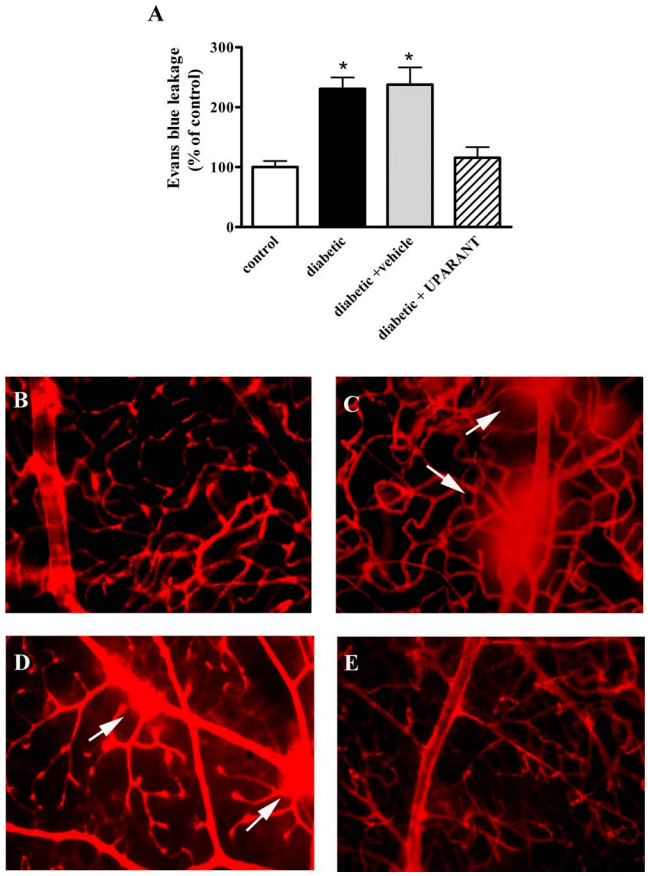

FIGURE 4. UPARANT reduces BRB breakdown. (**A**) Diabetes-induced leakage from the retina evaluated by the quantitative assessment of Evans blue dye extravasation. In diabetic rats untreated or vehicle-treated, the Evans blue leakage was higher than in controls. Daily dosing of UPARANT at 8 mg/kg for 5 days recovered this increase to a level close to that in controls (*$P < 0.001$ versus controls; ANOVA). Each column represents the mean ± SEM of data from six independent samples, each containing one retina. (**B**–**E**) Blood retinal vascular leakage as qualitatively evaluated with the Evans blue method in controls (**B**) and diabetic rats untreated (**C**), vehicle-treated (**D**), or treated with subcutaneous UPARANT (**E**). *Arrows*: vascular leakage. Six rats were used for each experimental condition. *Scale bar*: 200 μm.

UPARANT Effects on Pathologic Signs of DR

In the present study, UPARANT was administered at a dosage that was reduced by more than 50% with respect to the dose used in the PK study. This treatment was repeated daily, considering that repeated treatments are generally necessary to systemically deliver an adequate amount of a drug to the eye due to the presence of blood-ocular barriers.

ERG recording at different times after diabetes onset allows a longitudinal evaluation of retinal function during DR progression as well as the effects of therapeutic regimens. As shown by the present results, STZ causes reduction in a- and b-wave amplitude in agreement with previous findings in albino rats (for references, see Ref. 32). In contrast, no effects of STZ have been reported in pigmented rats,[24,25] suggesting that there may be different susceptibility to the effects of STZ in different strains and that albino rats may be more susceptible to retinal damage. We found that STZ induces a 50% reduction in both the photoreceptor and the inner retina response, although DR is generally thought to be an inner retinal disease and the b-wave seems to be involved earlier and more extensively than the a-wave.[26] On the other hand, recent findings suggest an early involvement of photoreceptors in DR[36] in line with our finding of a-wave reduction following STZ.

Here, UPARANT acts in a therapeutic regimen to counteract visual dysfunction, and its repeated administration is required to inhibit efficiently the production of those factors contributing to ERG dysfunction. In this line, repeated administration of a given compound is necessary to improve visual function after systemic drug delivery.[37–39] In STZ-rats, repeated administration of a traditional medicinal herb used in Chinese medicine recovers the amplitude of b-wave after 8 weeks, but not after 4 weeks.[40] After UPARANT withdrawal, ERG recovery lasts approximately 2 weeks, suggesting that following drug discontinuation, the ongoing hyperglycemia may reinstate the noxious environment causing the pathologic state of the retina. Similarly, in STZ-rats, ERG recovery after E4a, an analogue of the glucagon-like peptide 1 receptor, lasts 1 month after its withdrawal, but is lost after 3 months.[41]

Because any vascular change leading to reduced barrier properties can be detrimental for visual function,[27] therapeutic interventions aimed at restoring BRB integrity may have high impact in recovering ERG dysfunction as observed here after UPARANT. Indeed, we have found ameliorated BRB leakage after UPARANT inhibition of the uPA/uPAR system, which is in line with the fact that uPA/uPAR upregulation participates to BRB breakdown in DR.[9–11] In addition, UPARANT ameliorates BRB leakage by restoring altered levels of tight junction proteins in mouse models of either oxygen-induced retinopathy or AMD[20,22] and prevents the VEGF-induced permeability in a monolayer of human retinal endothelial cells.[16]

UPARANT Effects on Inflammatory and Vascular Responses

As demonstrated by the present results, UPARANT limits the production of inflammatory and proangiogenic factors, which codependently regulate processes playing a key role in the pathogenesis of DR.[42,43] Codependency of these factors is testified by a variety of studies showing, for instance, VEGF-dependent ICAM-1 expression leading to activation of leukocytes and the release of inflammatory cytokines[44] as well as cytokine production by Müller cells,[45] in which gliotic activation, with increased GFAP expression, is likely to contribute to BRB breakdown and vessel leakage.[46] In addition, IL-1β activates IL-6 production[47] and acts upstream of iNOS that participates to ICAM-1 upregulation and consequent diabetes-associated leukostasis.[48] Moreover, VEGF, IGF-1, FGF-2, and PDGF-B act synergistically on endothelial cells to induce vascular damage,[49] whereas VEGF expression and activity is known to be modulated by both IGF-1 and FGF-2.[50,51] Finally, together with VEGF, Ang-2 is recognized as a proangiogenic factor, but it also plays a role in inflammation,[6] being upregulated in response to hyperglycemia and leading to BRB breakdown through an action in combination with VEGF.[52]

The fact that the current therapeutic strategies in the management of DR have suboptimal efficacy may depend on their limited impact on inflammatory processes.[6] The present findings that UPARANT reduces the levels of inflammatory and proangiogenic factors are consistent with previous results in mouse models of neovascular diseases of the retina and the choroid,[20,22] suggesting UPARANT as a possible multitarget drug. This is in line with the finding that UPARANT counteracts the inflammatory and proangiogenic effects of the vitreous fluid from patients with proliferative DR, which contains high levels of several inflammatory and angiogenic factors.[22,53] In

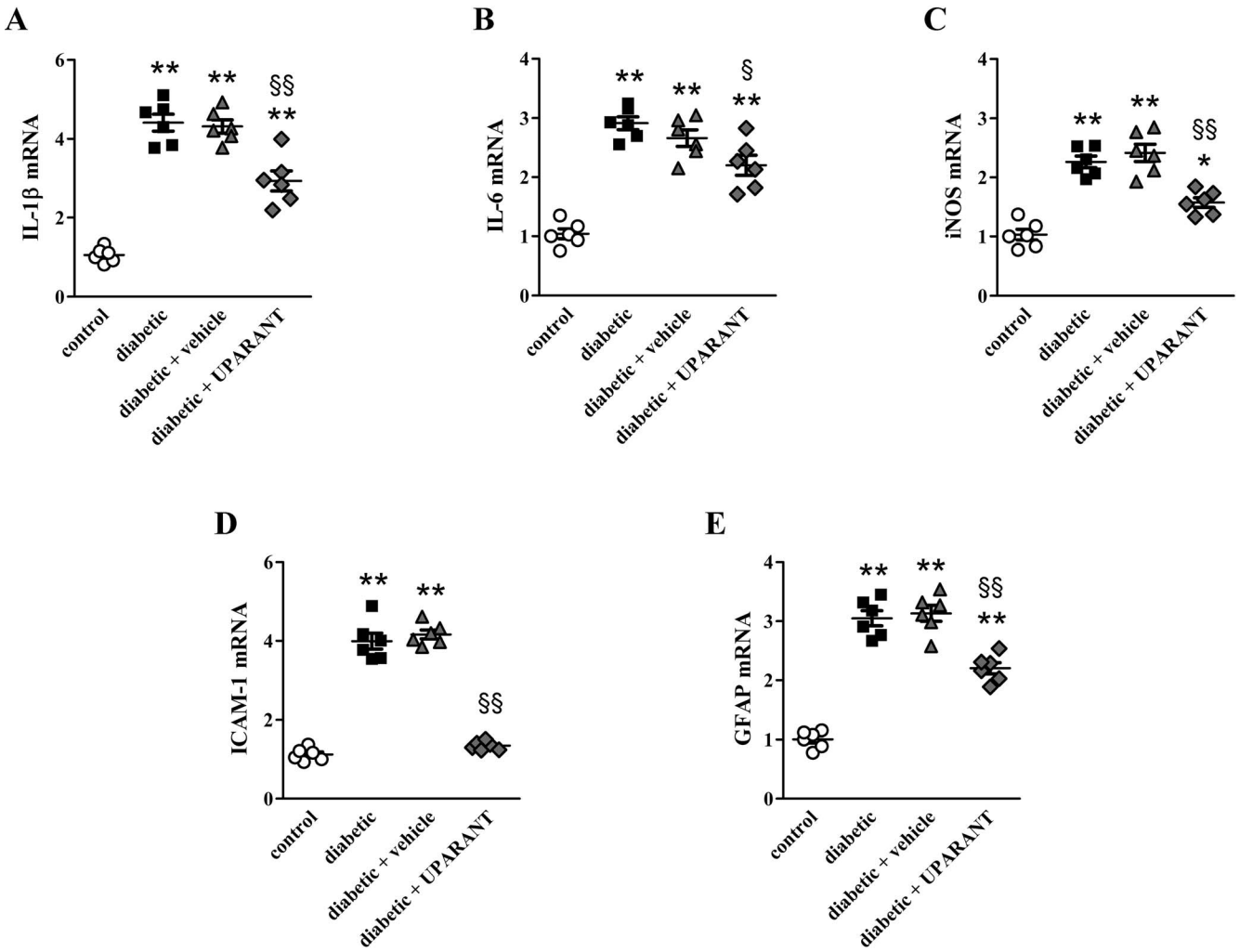

FIGURE 5. UPARANT reduces levels of inflammatory factors. Transcript levels of IL-1β (**A**), IL-6 (**B**), iNOS (**C**), ICAM-1 (**D**), and GFAP (**E**) were evaluated by relative quantification with qRT-PCR in controls and diabetic rats untreated, vehicle-treated, or treated with subcutaneous UPARANT at 8 mg/kg for 5 days. Data were analyzed by the formula $2^{-\Delta\Delta CT}$ using *18S* as the internal standard. In diabetic rats untreated or vehicle-treated, the levels of inflammatory factors were higher than in controls. Daily dosing of UPARANT reduced these levels, with a trend toward recovering those in controls ($^{*}P < 0.01$ and $^{**}P < 0.001$ versus controls; $^{\S}P < 0.05$ and $^{\S\S}P < 0.001$ versus vehicle-treated diabetic rats; ANOVA). Data are presented as scatter plots. Each plot represents the mean ± SEM of data from six independent samples, each containing one retina.

this respect, UPARANT inhibition of inflammation may have vascular benefits in DR much greater than most anti-VEGF therapies intended to regulate the vascular changes mediated by VEGF action without substantially intervening on inflammatory events.[54] Consistently, an important role of anti-inflammatory agents against the development and progression of DR lesions has been recently acknowledged.[55]

Efficacy of Subcutaneous Administration

As demonstrated here, subcutaneous UPARANT is effective in recovering diabetes-induced retinal injuries without producing significant damage to blood cells and systemic organs, thus supporting the concept that systemic treatment with UPARANT may be both effective and safe in the rat. With the exception of subcutaneous infusion of insulin, which is effective in slowing down DR in type 1 diabetic patients,[56] no subcutaneous drugs have been approved for treating retinopathies. On the other hand, in animal models, there is a considerable amount of data indicating that subcutaneous drug delivery is a promising route to access the posterior chamber of the eye, although little is known in DR. For instance, after 4 weeks from STZ injection, 5 days treatment with a bradykinin receptor B1 antagonist reduces early retinal alterations, including BRB breakdown.[57]

CONCLUSIONS

Together, the present findings support the possibility that uPAR activation participates with the mechanisms causing vascular damage in response to high glucose and provide evidence that the uPA/uPAR system is a promising target for the development of novel multitarget drugs in the treatment of early DR, therefore delaying the occurrence of late complications. The extrapolation of these experimental findings to the clinic is not straightforward, as animal models of DR may not faithfully recapitulate all the pathologic signs seen in human DR. In this respect, neither macular edema nor proliferative disease ever develop in STZ-rats, indicating that they are a

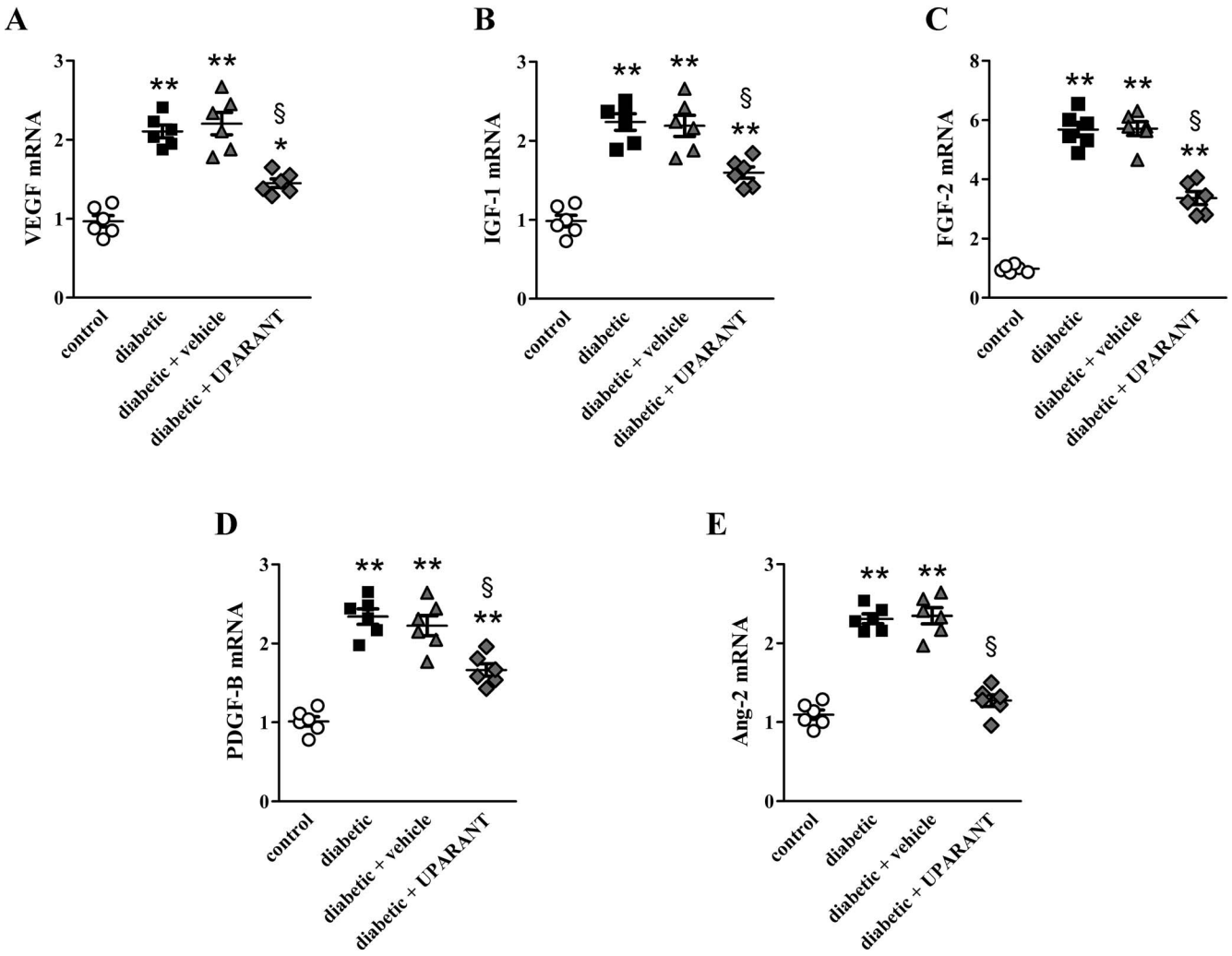

Figure 6. UPARANT reduces levels of proangiogenic factors. Transcript levels of VEGF (**A**), IGF-1 (**B**), FGF-2 (**C**), PDGF-B (**D**), and Ang-2 (**E**) were evaluated by relative quantification with qRT-PCR in controls and diabetic rats untreated, vehicle-treated, or treated with subcutaneous UPARANT at 8 mg/kg for 5 days. Data were analyzed by the formula $2^{-\Delta\Delta CT}$ using *18S* as the internal standard. In diabetic rats untreated or vehicle-treated, the levels of proangiogenic factors were higher than in controls. Daily dosing of UPARANT reduced these levels, with a trend toward recovering those in controls ($^{*}P < 0.01$ and $^{**}P < 0.001$ versus controls; $^{\S}P < 0.001$ versus vehicle-treated diabetic rats; ANOVA). Data are presented as scatter plots. Each plot represents the mean ± SEM of data from six independent samples, each containing one retina.

suitable model for the early phase of human DR, which is, however, often asymptomatic.

Acknowledgments

The authors thank Michele Ciccone for technical assistance in analytical method development and samples analysis. They also thank Daniela Pesce for the histologic evaluation of liver and kidney.

Supported by grants from the Italian Ministero della Salute (RF-201102351158; PB; Roma, Italy), BIOOS Italia (PB; Montegiorgio, Italy), European Union–Fondi Europei per lo Sviluppo Regionale, Italian Ministero dell'Istruzione e dell'Università, and the Italian Ministero dello Sviluppo Economico (PON01 02464; MDR and VP; Roma, Italy).

Disclosure: **M. Cammalleri**, None; **F. Locri**, None; **S. Marsili**, None; **M. Dal Monte**, None; **C. Pisano**, None; **A. Mancinelli**, None; **L. Lista**, None; **D. Rusciano**, BIOOS Italia (E); **M. De Rosa**, Pharmafelix (I), P; **V. Pavone**, Pharmafelix (I), P; **P. Bagnoli**, BIOOS Italia (F)

References

1. Zhang W, Liu H, Al-Shabrawey M, Caldwell RW, Caldwell RB. Inflammation and diabetic retinal microvascular complications. *J Cardiovasc Dis Res*. 2011;2:96–103.
2. Praidou A, Androudi S, Brazitikos P, Karakiulakis G, Papakonstantinou E, Dimitrakos S. Angiogenic growth factors and their inhibitors in diabetic retinopathy. *Curr Diabetes Rev*. 2010;6:304–312.
3. Qaum T, Xu Q, Joussen AM, et al. VEGF-initiated blood-retinal barrier breakdown in early diabetes. *Invest Ophthalmol Vis Sci*. 2001;42:2408–2413.
4. Dhoot DS, Avery RL. Vascular endothelial growth factor inhibitors for diabetic retinopathy. *Curr Diab Rep*. 2016;16:122.
5. Yu Y, Chen H, Su SB. Neuroinflammatory responses in diabetic retinopathy. *J Neuroinflammation*. 2015;12:141.
6. Rangasamy S, McGuire PG, Das A. Diabetic retinopathy and inflammation: novel therapeutic targets. *Middle East Afr J Ophthalmol*. 2012;19:52–59.

7. Shikari H, Silva PS, Sun JK. Complications of intravitreal injections in patients with diabetes. *Semin Ophthalmol*. 2014;29:276–289.
8. Shen Q, Wu JZ, Wong JC. Potential drug interventions for diabetic retinopathy. *Drug Discov Today*. 2013;18:1334–1341.
9. El-Remessy AB, Franklin T, Ghaley N, et al. Diabetes-induced superoxide anion and breakdown of the blood-retinal barrier: role of the VEGF/uPAR pathway. *PLoS One*. 2013;8:e71868.
10. Navaratna D, Menicucci G, Maestas J, Srinivasan R, McGuire P, Das A. A peptide inhibitor of the urokinase/urokinase receptor system inhibits alteration of the blood-retinal barrier in diabetes. *FASEB J*. 2008;22:3310–3317.
11. El-Remessy AB, Behzadian MA, Abou-Mohamed G, Franklin T, Caldwell RW, Caldwell RB. Experimental diabetes causes breakdown of the blood-retina barrier by a mechanism involving tyrosine nitration and increases in expression of vascular endothelial growth factor and urokinase plasminogen activator receptor. *Am J Pathol*. 2003;162:1995–2004.
12. Eden G, Archinti M, Furlan F, Murphy R, Degryse B. The urokinase receptor interactome. *Curr Pharm Des*. 2011;17:1874–1889.
13. Sugioka K, Kodama A, Okada K, et al. TGF-β2 promotes RPE cell invasion into a collagen gel by mediating urokinase-type plasminogen activator (uPA) expression. *Exp Eye Res*. 2013;115:13–21.
14. Elner SG, Elner VM, Kindzelskii AL, et al. Human RPE cell lysis of extracellular matrix: functional urokinase plasminogen activator receptor (uPAR), collagenase and elastase. *Exp Eye Res*. 2003;76:585–595.
15. Das A, McGuire PG, Eriqat C, et al. Human diabetic neovascular membranes contain high levels of urokinase and metalloproteinase enzymes. *Invest Ophthalmol Vis Sci*. 1999;40:809–813.
16. Motta C, Lupo G, Rusciano D, et al. Molecular mechanisms mediating antiangiogenic action of the urokinase receptor-derived peptide UPARANT in human retinal endothelial cells. *Invest Ophthalmol Vis Sci*. 2016;57:5723–5735.
17. Yang J, Caldwell RB, Behzadian MA. Blockade of VEGF-induced GSK/β-catenin signaling, uPAR expression and increased permeability by dominant negative p38α. *Exp Eye Res*. 2012;100:101–108.
18. Yang J, Duh EJ, Caldwell RB, Behzadian MA. Antipermeability function of PEDF involves blockade of the MAP kinase/GSK/beta-catenin signaling pathway and uPAR expression. *Invest Ophthalmol Vis Sci*. 2010;51:3273–3280.
19. Behzadian MA, Windsor LJ, Ghaly N, Liou G, Tsai NT, Caldwell RB. VEGF-induced paracellular permeability in cultured endothelial cells involves urokinase and its receptor. *FASEB J*. 2003;17:752–754.
20. Cammalleri M, Dal Monte M, Locri F, et al. The urokinase receptor-derived peptide UPARANT mitigates angiogenesis in a mouse model of laser-induced choroidal neovascularization. *Invest Ophthalmol Vis Sci*. 2016;57:2586–2597.
21. Carriero MV, Bifulco K, Minopoli M, et al. UPARANT: a urokinase receptor-derived peptide inhibitor of VEGF-driven angiogenesis with enhanced stability and in vitro and in vivo potency. *Mol Cancer Ther*. 2014;13:1092–1104.
22. Dal Monte M, Rezzola S, Cammalleri M, et al. Antiangiogenic effectiveness of the urokinase receptor-derived peptide UPARANT in a model of oxygen-induced retinopathy. *Invest Ophthalmol Vis Sci*. 2015;56:2392–2407.
23. Kusari J, Zhou S, Padillo E, Clarke KG, Gil DW. Effect of memantine on neuroretinal function and retinal vascular changes of streptozotocin-induced diabetic rats. *Invest Ophthalmol Vis Sci*. 2007;48:5152–5159.
24. Aung MH, Kim MK, Olson DE, Thule PM, Pardue MT. Early visual deficits in streptozotocin-induced diabetic long evans rats. *Invest Ophthalmol Vis Sci*. 2013;54:1370–1377.
25. Ramsey DJ, Ripps H, Qian H. An electrophysiological study of retinal function in the diabetic female rat. *Invest Ophthalmol Vis Sci*. 2006;47:5116–5124.
26. Li Q, Zemel E, Miller B, Perlman I. Early retinal damage in experimental diabetes: electroretinographical and morphological observations. *Exp Eye Res*. 2002;74:615–625.
27. Klaassen I, Van Noorden CJ, Schlingemann RO. Molecular basis of the inner blood-retinal barrier and its breakdown in diabetic macular edema and other pathological conditions. *Prog Retin Eye Res*. 2013;34:19–48.
28. Reagan-Shaw S, Nihal M, Ahmad N. Dose translation from animal to human studies revisited. *FASEB J*. 2008;22:659–661.
29. Naka KI, Rushton WA. S-potentials from colour units in the retina of fish (Cyprinidae). *J Physiol* 1966;1:536–555.
30. Kovacs B, Lumayag S, Cowan C, Xu S. MicroRNAs in early diabetic retinopathy in streptozotocin-induced diabetic rats. *Invest Ophthalmol Vis Sci*. 2011;52:4402–4409.
31. U.S. Department of Health and Human Services, Food and Drug Administration, Center for Drug Evaluation and Research. Guidance for industry, bioanalytical method validation. Silver Spring, MD: U.S. Department of Health and Human Services, Food and Drug Administration, Center for Drug Evaluation and Research; 2001. Available at https://www.fda.gov/downloads/Drugs/Guidance/ucm070107.pdf. Accessed June 8, 2017.
32. Miranda M, Sánchez-Villarejo MV, Álvarez-Nölting R, Vilela C, Romero FJ. Electroretinogram alterations in diabetes? In: Belusic G, ed. *Electroretinograms*. Rijeka, Croatia: InTech; 2011:157–172.
33. Gaudana R, Ananthula HK, Parenky A, Mitra AK. Ocular drug delivery. *AAPS J*. 2010;12:348–360.
34. Zhang SX, Sima J, Shao C, et al. Plasminogen kringle 5 reduces vascular leakage in the retina in rat models of oxygen-induced retinopathy and diabetes. *Diabetologia*. 2004;47:124–131.
35. Breuss JM, Uhrin P. VEGF-initiated angiogenesis and the uPA/uPAR system. *Cell Adh Migr*. 2012;6:535–615.
36. Liu H, Tang J, Du Y, et al. Photoreceptor cells influence retinal vascular degeneration in mouse models of retinal degeneration and diabetes. *Invest Ophthalmol Vis Sci*. 2016;57:4272–4281.
37. Ranchon I, Chen S, Alvarez K, Anderson RE. Systemic administration of phenyl-N-tert-butylnitrone protects the retina from light damage. *Invest Ophthalmol Vis Sci*. 2001;42:1375–1379.
38. Dal Monte M, Latina V, Cupisti E, Bagnoli P. Protective role of somatostatin receptor 2 against retinal degeneration in response to hypoxia. *Naunyn Schmiedebergs Arch Pharmacol*. 2012;385:481–494.
39. Martini D, Dal Monte M, Ristori C, et al. Antiangiogenic effects of β2-adrenergic receptor blockade in a mouse model of oxygen-induced retinopathy. *J Neurochem*. 2011;119:1317–1329.
40. Wang Y, Qin S, Pen G, et al. Original research: potential ocular protection and dynamic observation of Polygonatum sibiricum polysaccharide against streptozocin-induced diabetic rats' model. *Exp Biol Med (Maywood)*. 2017;242:92–101.
41. Zhang Y, Zhang J, Wang Q, et al. Intravitreal injection of exendin-4 analogue protects retinal cells in early diabetic rats. *Invest Ophthalmol Vis Sci*. 2011;52:278–285.
42. Roy S, Kern TS, Song B, Stuebe C. Mechanistic insights into pathological changes in the diabetic retina: implications for targeting diabetic retinopathy. *Am J Pathol*. 2017;187:9–19.
43. Romero-Aroca P, Baget-Bernaldiz M, Pareja-Rios A, Lopez-Galvez M, Navarro-Gil R, Verges R. Diabetic macular edema pathophysiology: vasogenic versus inflammatory. *J Diabetes Res*. 2016;2016:2156273.
44. Kern TS. Contributions of inflammatory processes to the development of the early stages of diabetic retinopathy. *Exp Diabetes Res*. 2007;2007:95103.

Investigative Ophthalmology & Visual Science

45. Sorrentino FS, Allkabes M, Salsini G, Bonifazzi C, Perri P. The importance of glial cells in the homeostasis of the retinal microenvironment and their pivotal role in the course of diabetic retinopathy. *Life Sci*. 2016;162:54–59.
46. Bringmann A, Pannicke T, Grosche J, et al. Müller cells in the healthy and diseased retina. *Prog Retin Eye Res*. 2006;25:397–424.
47. Liu X, Ye F, Xiong H, et al. IL-1β induces IL-6 production in retinal Müller cells predominantly through the activation of P38 MAPK/NF-kB signaling pathway. *Exp Cell Res*. 2015;331:223–231.
48. Tang J, Kern TS. Inflammation in diabetic retinopathy. *Prog Retin Eye Res*. 2011;30:343–358.
49. Simó R, Carrasco E, García-Ramírez M, Hernández C. Angiogenic and antiangiogenic factors in proliferative diabetic retinopathy. *Curr Diabetes Rev*. 2006;2:71–98.
50. Presta M, Andrés G, Leali D, Dell'Era P, Ronca R. Inflammatory cells and chemokines sustain FGF2-induced angiogenesis. *Eur Cytokine Netw*. 2009;20:39–50.
51. Ruberte J, Ayuso E, Navarro M, et al. Increased ocular levels of IGF-1 in transgenic mice lead to diabetes-like eye disease. *J Clin Invest*. 2004;113:1149–1157.
52. Rangasamy S, Srinivasan R, Maestas J, McGuire PG, Das A. A potential role for angiopoietin 2 in the regulation of the blood-retinal barrier in diabetic retinopathy. *Invest Ophthalmol Vis Sci*. 2011;52:3784–3791.
53. Rezzola S, Corsini M, Chiodelli P, et al. Inflammation and N-formyl peptide receptors mediate the angiogenic activity of human vitreous humour in proliferative diabetic retinopathy. *Diabetologia*. 2017;60:719–728.
54. Arimura N, Otsuka H, Yamakiri K, et al. Vitreous mediators after intravitreal bevacizumab or triamcinolone acetonide in eyes with proliferative diabetic retinopathy. *Ophthalmology*. 2009;116:921–926.
55. Das A, McGuire PG, Monickaraj F. Novel pharmacotherapies in diabetic retinopathy: Current status and what's in the horizon? *Indian J Ophthalmol*. 2016;64:4–13.
56. Zabeen B, Craig ME, Virk SA, et al. Insulin pump therapy is associated with lower rates of retinopathy and peripheral nerve abnormality. *PLoS One*. 2016;11:e0153033.
57. Catanzaro O, Labal E, Andornino A, Capponi JA, Di Martino I, Sirois P. Blockade of early and late retinal biochemical alterations associated with diabetes development by the selective bradykinin B1 receptor antagonist R-954. *Peptides*. 2012;34:349–352.

Investigative Ophthalmology & Visual Science